Available online at www.sciencedirect.com

ScienceDirect

Energy Procedia 82 (2015) 424 – 431

Energy Procedia

ATI 2015 - 70th Conference of the ATI Engineering Association

Combustion CFDmodelingof a spark ignited optical access engine fueled with gasoline and ethanol

Michele Battistoni[a], Francesco Mariani[a]*, Francesco Risi[a], Claudio Poggiani[a]

[a]*University of Perugia, Department of Engineering, via G. Duranti, 63, 06125, Perugia, Italy*

Abstract

In this study we present the Computational Fluid Dynamics (CFD) modeling of the combustion process using detailed chemistry in a spark-ignited (SI) optical access engine operated at part load using gasoline and ethanol as fuels. Simulation results are comparedagainst experimental optical and indicating data. The engine is installed at the Department of Engineering of the University of Perugia, and it features a four-valve head, a transparent flat piston and a port-fuel-injection (PFI) system. Full open cycle simulations have been performed using the commercial code CONVERGE. The combustion process has been simulated using detailed chemistry and adaptive mesh refinement (AMR) to resolve in detail and track the reaction zone, in a Reynolds Averaged Navier-Stokes (RANS) modeling framework. In-cylinder pressure, heat release, and flame morphology have been compared with experimental indicating and imaging data. Tests and simulations span different air-fuel ratios in lean and rich conditions (relative air-fuel ratio λranges from 0.9 to 1.1).Results indicate that simulations are able to predict experimental data with high accuracy. Variations due to changing fuel type and air-fuel ratio are well captured. The computational cost to achieve grid-independent results has been evaluated and it is also not excessively high. Taking into account that the engine speed was quite low, i.e., 900 rpm, we conclude that, in this condition, detailed chemistry coupled with RANS works satisfactorily without turbulence chemistry interaction sub-models, and therefore without any tunings.

Peer-review under responsibility of the Scientific Committee of ATI 2015

Keywords: optical access engine; SI combustion; ethanol; gasoline; CFD simulation; detailed chemistry

1. Introduction

Alternative liquid fuels represent one of the leading research topics for the current development of engines in the transportation sector [1-3]. The continuous reductionof CO_2emission limitsispushing spark ignition engines towards downsizing, turbocharging, and direct injection. These technologies arebetter enabled by the usage of knock-resistant fuels, which are obtained when low carbon number alcohols, like

* Corresponding author. Tel.: +39-075-585-3732
E-mail address: francesco.mariani@unipg.it

Peer-review under responsibility of the Scientific Committee of ATI 2015
doi:10.1016/j.egypro.2015.11.829

methanol or ethanol, are blended with gasoline. The advantages arealso due to their higher heat of vaporization which cools down the charge,andto theirlower air-to-fuel ratio.Such alcohols are also attractive because they can be produced from renewable sources.In addition, liquid fuels take advantage of high energy density, ease of storage, and usage of existing infrastructure for their distribution.Therefore, the alcohol pathway is already in place in many countriesand is very attractive compared to alternative mobility technologies such as electric vehicles and hydrogen vehicles, which may not scale sustainably beyond the level of a niche market in the foreseeable future [2].

Fuel effects can be conveniently and deeply investigated through optical access engines, as these can enable or enhance the observation of many important phenomena, concerning sprays, mixing and combustion development.[4-6]. Focusing only on the combustion behavior, several authors [7,8] reported that an external mixture preparation system allows a decoupling of injection and spray phenomena from the combustion. Direct fuel injection(DI) obviously causes complex mixing processes, and also introduces some variability due to details on injector manufacturing, mounting or operation. PFI fueling, on the contrary, reduces uncertainties when fuel effects on combustion are investigated. Following these guidelines, the present work makes use of a PFI system for comparing gasoline and ethanol behaviors.

From a simulation perspective, SI engine combustion is still generally modeled under the RANS approach mainly because it is computationally cheap, even if Large Eddy Simulations (LES) are rapidly becoming more affordable. Turbulence effects, which are not directly solved, are usually modeled by enhancing viscosity to account for either the fluctuating velocity (in RANS) or the sub-grid velocity (in LES).Combustion at a fundamental level is governed by two phenomena, i.e., mixing (of species, energy, and momentum) and chemical reactions. The enhanced mixing is accounted for by the turbulence model itself. Chemical reaction rates, which depend at a molecular level on species concentration and temperature according to Arrhenius equation, are modeled as source terms in the species transport equation. In a turbulent field, however, the local averaged reaction rate differs from the rate evaluated at the average temperature, as temperature effects are extremely nonlinear(i.e., the source term does not commute) [9]. A tremendous amount of research deals with turbulent combustion modeling to make up for these effects, which are generally referred to as turbulence-chemistry interaction (TCI) models [9,10,11]. Nevertheless, when detailed chemistry is directly coupled to RANS by treating each cell as a well-stirred (or well-mixed) reactor and it is supported by a local fine grid, several authors have reported good results in compression and also in spark ignition engine applications without using any additional TCI models [12,13, 14].

Following these considerations, in the present study, we simulated pure gasoline and pure ethanol combustion in a 4-valve single-cylinder SI engine. Since fueling is provided by a PFI system, we assumed premixed combustion conditions and used detailed chemistry with the well-mixed combustion model approach. Simulation results are comparedwith data from optical engine experiments. The objectives were primarily the assessment of the simulation methodology with detailed chemistry for this SI optical engine setup, and secondarily the evaluation of the flame morphology for each fuel at different air-fuel ratios.

2. Engine description and experimental data

The optical engine is showninFig.1 and its main features are given in Table 1. It is a 500 cm3 single cylinder engine with pent-roof combustion chamber, four valves and reverse tumble intake port design [15]. It can feature both direct injection (GDI) and port fuel injection (PFI). The engine is also equipped with a camless electro-hydraulic VVA system that allows free control of valve timing and lift [16,17]. The combustion chamber is optically accessible through a 60 mm diameter quartz piston crown window, in conjunction with an extended piston and a stationary 45° mirror. Piston-liner contact uses dry lubrication

to allow clean visualization in the combustion chamber, therefore conventional piston rings are replaced with graphite rings. In this study the PFI system is used. Indicated analysis is carried out based on data from a piezoelectric pressure transducer mounted on one side of the chamber, a piezoresistive pressure transducer mounted on the intake port for pegging, and an optical encoder operated at 0.2 CAD resolution. Flame images are recorded using a PCO Flash-cam CCD camera, with 636x576 pixel image resolution [15].

3. Computational methodology

In this work, the CONVERGE CFD software package [18,19] is used as the computational framework for running the simulations. The code allows the calculation of the three-dimensional, compressible, chemically-reacting fluid flows in complex geometries with moving boundaries, and it is specifically tailored for piston engine analysis. The code uses a modified cut-cell Cartesian method that eliminates the need for the computational grid to be morphed with the geometry of interest, while still precisely represents the true boundary shape. This approach allows for the use of simple orthogonal grids, and completely automates the mesh generation process. Fig. 2 shows the domain used for the simulations (Fig. 2.a). Fixed embedding is used in the cylinder and in the valve seat regions. Temperature based adaptive mesh refinement (AMR) is used to resolve the flame front during the combustion (Fig. 2.b), and velocity based AMR is used elsewhere to resolve complex flow structures. Table 2 provides details on the grids used.

The optical access engine is simulated at 900 rpm, with three relative air-fuel ratios (λ = 0.9, 1.0 and 1.1) and two fuels, standard European gasoline and pure ethanol. The modeling approach is based on the unsteady Reynolds Averaged Navier-Stokes (RANS) equations, using the Re-Normalization Group (RNG) k-ε turbulence model, and the well-mixed approach for the combustion. Detailed chemistry is used for each fuel without any turbulence-chemistry interaction model. This approach relies on the fine resolution of the reaction zone, achieved with the AMR. A multi-zone approach is also used to accelerate the calculation of the chemical kinetics. In this respect, temperature and equivalence ratio bin sizes have been set to 5 K and 0.05, respectively.

Gasoline chemical kinetics has been modeled using the reduced mechanism based on the work of Liu et al. [20] for the primary reference fuels iso-octane and n-heptane, consisting of 48 species and 152 reactions. Ethanol oxidation is based on the detailed mechanism for low carbon atoms hydrocarbon developed by Ranzi et al. [21] consisting of 107 species and 2642 reactions.

Combustion is initiated by an energy deposition method, sourcing the energy equation with 20 mJ for 0.5 CAD (simulating the arc phase), and with additional 20 mJ for 10 CAD (simulating the glow phase). Spark timing is fixed and set to -17 CAD a TDC as in the experiments. The grid resolution around the electrodes is refined with two concentric spherical embedding (cf. Table 2).

Fuel injection is not modeled directly, but a premixed air-fuel mixture is admitted from the inlet boundary simulating a prefect mixing of the fuel vapor and air. Also, fuel and air are perfectly mixed initially in the intake port. The engine is operated at part load, and the throttle is included in the 3D domain, as visible in Fig. 2.a. Boundary conditions, consisting basically of static pressure and temperature for the inflow, and static pressure for the outflow, have been derived from experiments. Simulations are run for one engine cycle starting from -450 CAD, i.e., during the exhaust phase, and extending up to 270 CAD a TDC.

Table 1. Engine data and operating conditions.

Data	Value
Bore [m]	0.085
Stroke [m]	0.088
Connecting rod length [m]	0.139
Compression ratio	8.8
Intake Valve Open/Close [CAD a TDC firing]	-394 / -161
Exhaust Valve Open/Close [CAD a TDC firing]	-567 / -335
Engine speed [rpm]	900
Fuels	Gasoline / Ethanol
Spark timing [CAD a TDC firing]	-17
Relative air-fuel ratio, λ	0.9 / 1.0 / 1.1
Injection	PFI
Indicated Mean Effective Pressure [bar]	~7

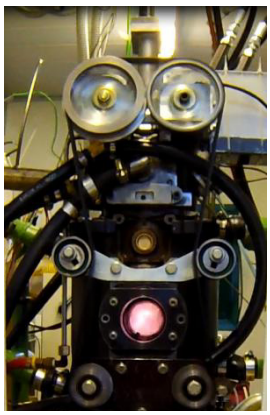

Fig. 1. Optical access engine in firing condition.

Table 2. Mesh details.

base grid size [mm] (embedding level 0)	temperature and velocity based AMR cell size [mm] (embedding level 3)	spark electrodes cell size [mm] (embedding level 5)	minimum and peak cell count
8.0	**1.0**	0.25	150,000 to 450,000
6.0	**0.75**	0.1875	300,000 to 900,000
5.0	**0.625**	0.15625	500,000 to 1,400,000

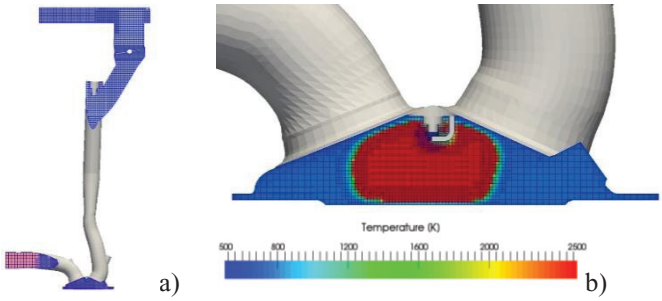

Fig. 2. Global engine view with intake and exhaust ports - inlet plenum and exhaust pipe are clipped in the figure (a). Combustion chamber cut plane showing flame front resolved using temperature AMR (b).

4. Results and discussion

4.1. Mesh sensitivity study

As discussed in the Introduction section, in a premixed case, combustion is controlled by mixing and by chemical reaction rates. An important aspect when detailed chemistry is directly used in a RANS framework is the so called "commutation" error of the chemical source term. There is no guarantee that the RANS averaged chemical source term equals the chemical source term evaluated with the RANS averaged temperature and species mass fractions. Due to the strong temperature non-linearity in the reaction rates, there is an approximation assuming that the RANS averaging commutes. However, in RANS, where mixing is enhanced by turbulence through the turbulent viscosity, it is important to check that the averaged flow field is well resolved, so that any commutation error be as small as possible or irrelevant.

The effects of the grid size on the combustion are shown in Fig. 3 with reference to the gasoline fuel case at λ =1. The in-cylinder pressure curves and burn rates show that a satisfactory grid convergence is achieved as the AMR grid size, which is mainly active across the flame front, reaches 0.75 mm. A finer grid size seems not to add much in this case. The predicted pressure trace agrees very well with the measured curve, taking also into account that the blow-by is exacerbated in the optical engine setup. The role of the modeled turbulence can be appreciated on the right side of Fig. 3. Combustion is grid-converged when the modeled turbulent kinetic energy (TKE) or turbulent length-scale values are also converged. It is worth noting that the modeled length-scale (averaged over the chamber volume) reaches values of about 0.25 mm which is well below the AMR grid size used. This suggests that further improvements or better grid-converged results are to be expected if a much finer grid could be used. However, the reduction of the AMR grid size down to 0.25 mm would roughly mean a two orders of magnitude increase in the computational cost compared to the 0.75 mm. This is beyond the scope of this work, and given the good results already achieved at 0.75 mm, the latter has been considered adequate and used for the rest of the study.

It is also worth noting that in our case the cell size required for grid-converged results seem not to be excessively severe, as found instead in other works [12,22]: this might be due, among other factors, to the quite low engine speed that has been tested (900 rpm) which determines a mild turbulence intensity level in the chamber.

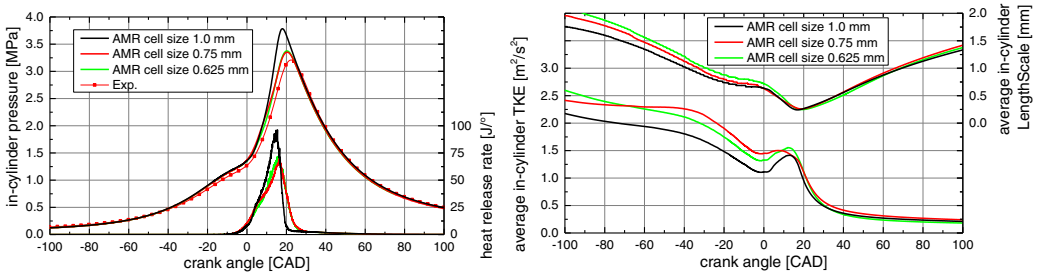

Fig. 3. Mesh sensitivity (gasoline fuel, $\lambda = 1$)

4.2. Air-fuel ratio and fuel type effects

The main focus of this paper is the comparison of ethanol and is o-octane combustion behaviors under the optical engine test conditions. The results of air-fuel ratio effect on in-cylinder pressure and heat release rate are shown in Fig. 4.a. As expected, as the mixture gets richer the combustion progress accelerates. Thebehavior is very well reproduced by the simulations, both in terms of absolute values as well as in terms of sensitivity to λ values. The reduced mechanisms of Liu et al. [21] proved to be robust and accurate. Combustion phasing is well captured, and peak pressure is slightly overestimated only for the rich case. Ethanol behaves in a similar manner with respect to the air-fuel ratio, but plots are not shown for brevity.

As far as fuel type effects are concerned, the in-cylinder pressure traces and heat release rates are shown in Fig. 4.b for the cases with $\lambda = 1$.The predicted ethanol combustion rate is faster than the corresponding gasoline rate, in agreement with the experiments. The combustion speed differences between the two fuels are marginally larger in the simulations, than in the experiments. The detailed combustion mechanism by Ranzi et al. [22] combined with ARM performed satisfactorily in the cases tested.

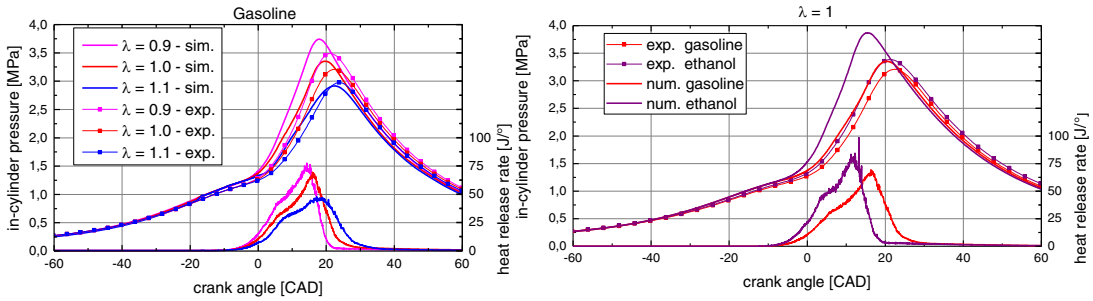

Fig. 4. (a) Air-fuel ratio effect, using gasoline fuel; (b) Fuel effect, at $\lambda = 1$.

Lastly, a quick overview of the flame development is given in Fig. 5 for gasoline and ethanol in rich conditions, ($\lambda = 0.9$). Flames are visualized with iso-surfaces of T=2000 K and reported every 6° for five different timings after the spark event. Experimental images are available for the first two time instances. The faster growth of the ethanol is well visible. Initially the flame is slightly convected towards the exhaust valves as a result of some residual charge motion. Another notable feature is that the main expansion is along the chamber roof edge, as expected for the larger volume available.

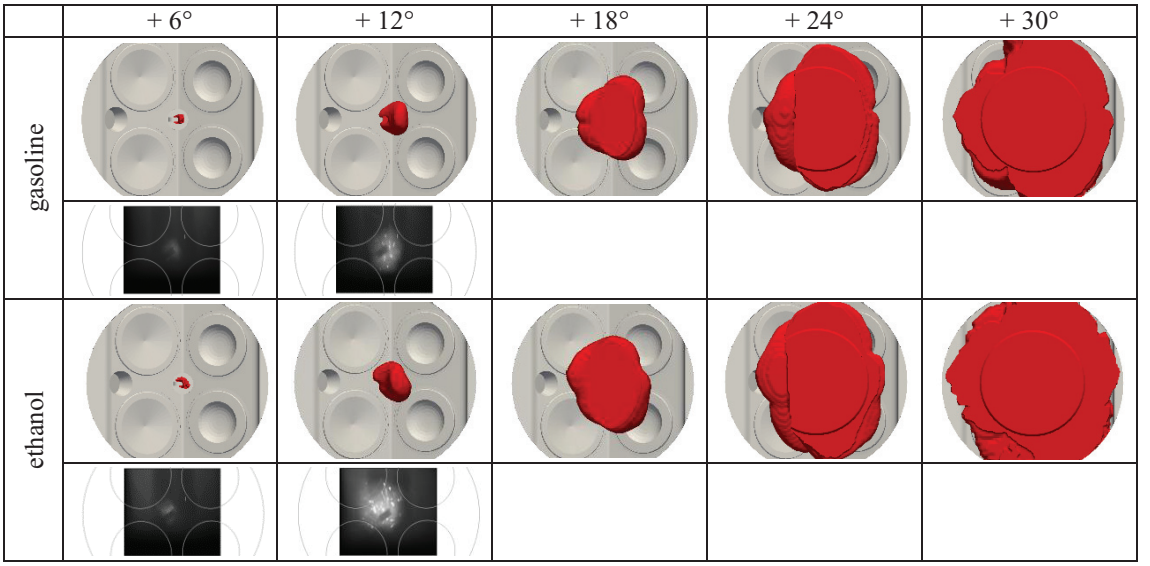

Fig. 5. Flame front images ($\lambda = 0.9$), gasoline top row, ethanol bottom row. Crank angles are given after ignition timing.

5. Conclusions

The study presents a simulation work aimed at predicting the combustion behavior in an optical access SI engine fueled with gasoline and ethanol. Ethanol and gasoline combustion speed, at various air-fuel ratios are well described by the model.

The work shows that in the tested conditions accurate results can be achieved directly using detailed chemistry, with a RANS turbulence model and a reasonably fine grid in the reaction zone, by means of AMR. Predictions are in good agreement with measurements without tuning. Enhance turbulent mixing is accounted for by the turbulence model, while the commutation error, even if not eliminated and not addressed, does not seem to have a significant impact on the results.

References

1. Sarathy S.M., Oßwald P., Hansen N., Kohse-Höinghaus K., “Alcohol combustion chemistry”, *Progress in Energy and Combustion Science*, 44 (2014) 40-102.

2. Sileghem, L., Ickes, A., Wallner, T., and Verhelst, S., "Experimental Investigation of a DISI Production Engine Fuelled with Methanol, Ethanol, Butanol and ISO-Stoichiometric Alcohol Blends," SAE Technical Paper 2015-01-0768, (2015).

3. Fraioli V., Mancaruso E., Migliaccio M., Vaglieco B.M., “Ethanol effect as premixed fuel in dual-fuel CI engines: Experimental and numerical investigations“, *Applied Energy* 119 (2014) 394–404.

4. Storch M., Erdenkäufer S., Wensing M., Will S., Zigan L., “The Effect of Ethanol Blending on Combustion and Soot Formation in an Optical DISI Engine Using High-Speed Imaging”, *Energy Procedia* 66 (2015) 77-80.

5. Price, P., Stone, R., Collier, T., and Davies, M., "Particulate Matter and Hydrocarbon Emissions Measurements: Comparing First and Second Generation DISI with PFI in Single Cylinder Optical Engines," SAE Technical Paper 2006-01-1263, (2006).

6. Aleiferis, P.G., Serras-Pereira, J., Richardson, D., "Characterization of flame development with ethanol, butanol, iso-octane, gasoline and methane in a direct-injection spark-ignition engine", *Fuel*, 109 (2013) 256-278.

7. Zhu, G., Stuecken, T., Schock, H., Yang, X. et al., "Combustion Characteristics of a Single-Cylinder Engine Equipped with Gasoline and Ethanol Dual-Fuel Systems," SAE Technical Paper 2008-01-1767, (2008).

8. Aleiferis, P., Malcolm, J., Todd, A., Cairns, A. et al., "An Optical Study of Spray Development and Combustion of Ethanol, Iso-Octane and Gasoline Blends in a DISI Engine," SAE Technical Paper 2008-01-0073, (2008).

9. Fox R.O., "Computational Models for Turbulent Reacting Flows", Cambridge University Press, (2003).

10. Peters N., "Turbulent Combustion", Cambridge University Press, (2000).

11. Colin, O., and Benkenida, A., "The 3-Zones Extended Coherent Flame Model (ECFM3Z) for Computing Premixed/Diffusion Combustion," *Oil & Gas Science and Technology*, 59, 6, 593-609, (2004).

12. Pomraning, E., Richards, K., and Senecal, P., "Modeling Turbulent Combustion Using a RANS Model, Detailed Chemistry, and Adaptive Mesh Refinement," SAE Technical Paper 2014-01-1116, (2014).

13. Givler, S., Raju, M., Pomraning, E., Senecal, P. et al., "Gasoline Combustion Modeling of Direct and Port-Fuel Injected Engines using a Reduced Chemical Mechanism," SAE Technical Paper 2013-01-1098, (2013).

14. Puduppakkam, K., Naik, C., Meeks, E., Krenn, C. et al., "Predictive Combustion and Emissions Simulations for a High Performance Diesel Engine Using a Detailed Fuel Combustion Model," SAE Technical Paper 2014-01-2570, (2014).

15. Donadio G., Poggiani C., Rondoni L., Grimaldi C.N., De Cesare M., Bellato N., "Combustion Analysis in an Optical Access Engine", *Energy Procedia*, 45 (2014) 959-966.

16. Battistoni, M., Mariani, F., Foschini, L., and Cristiani, M., "A Parametric Optimization Study of a Hydraulic Valve Actuation System," SAE Int. J. Engines 1(1):970-984, (2009).

17. Postrioti, L., Battistoni, M., Foschini, L., and Flora, R., "Application of a Fully Flexible Electro-Hydraulic Camless System to a Research SI Engine," SAE Technical Paper 2009-24-0076, (2009).

18. Richards, K. J., Senecal, P. K., and Pomraning, E. CONVERGE v.2.2 Documentation. Convergent Sciences Inc, (2014).

19. Senecal, P., Richards, K., Pomraning, E., Yang, T. et al., "A New Parallel Cut-Cell Cartesian CFD Code for Rapid Grid Generation Applied to In-Cylinder Diesel Engine Simulations," SAE Technical Paper 2007-01-0159, (2007).

20. Liu, Y., Jia, M., Xie, M. and Pang, B., "Enhancement of a Skeletal Kinetic Model for Primary Reference Fuel Oxidation by Using a Semidecoupling Methodology," *Energy Fuels*, (2012), 26 (12), pp 7069–7083.

21. Ranzi E., Frassoldati A., Grana R., Cuoci A., Faravelli T., Kelley A.P., Law C.K., Hierarchical and comparative kinetic modeling of laminar flame speeds of hydrocarbon and oxygenated fuels, *Progress in Energy and Combustion Science*, 38 (4), pp. 468-501 (2012).

22. Senecal, P., Pomraning, E., Richards, K., and Som, S., "An Investigation of Grid Convergence for Spray Simulations using an LES Turbulence Model," SAE Technical Paper 2013-01-1083, (2013).

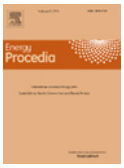

Biography

Francesco Mariani, since 2001AssociateProfessor of Machinery and Energy Systems. Author of 70 scientific papers. Research topics: CFD-3D analysis of ICE, sprays, cavitation, combustion, non-conventional fuels.1D-3D coupling. Gas-solid multiphase systems. External fluid-dynamics. Diagnosis and monitoring coupling neural and expert systems.